Neurobiology of Aging xxx (2015) 1–13

Contents lists available at ScienceDirect

Neurobiology of Aging

journal homepage: www.elsevier.com/locate/neuaging

The CCAAT/enhancer-binding protein delta/miR135a/thrombospondin 1 axis mediates PGE2-induced angiogenesis in Alzheimer's disease

Chiung-Yuan Ko [a,b], Yu-Yi Chu [c], Shuh Narumiya [d], Jhih-Ying Chi [e], Tomoyuki Furuyashiki [d], Tomohiro Aoki [d], Shao-Ming Wang [e], Wen-Chang Chang [f], Ju-Ming Wang [c,e,f,g,*]

[a] Ph.D. Program for Neural Regenerative Medicine, College of Medical Science and Technology, Taipei Medical University, Taipei, Taiwan
[b] Center for Neurotrauma and Neuroregeneration, Taipei Medical University, Taipei, Taiwan
[c] Institute of Bioinformatics and Biosignal Transduction, National Cheng Kung University, Tainan, Taiwan
[d] Core Research for Evolutional Science and Technology (CREST), Kyoto, Japan
[e] Institute of Basic Medical Sciences, National Cheng Kung University, Tainan
[f] Graduate Institute of Medical Sciences, College of Medicine, Taipei Medical University, Taipei, Taiwan
[g] Infectious Disease and Signaling Research Center, National Cheng Kung University, Tainan, Taiwan

ARTICLE INFO

Article history:
Received 27 March 2014
Received in revised form 30 September 2014
Accepted 25 November 2014

Keywords:
Alzheimer's disease
PGE2
Angiogenesis
miRNA
CEBPD

ABSTRACT

In Alzheimer's disease (AD), large populations of endothelial cells undergo angiogenesis due to brain hypoxia and inflammation. Substantial evidence from epidemiologic, pathologic, and clinical reports suggests that vascular factors are critical for the pathogenesis of AD. However, the precise mechanistic correlation between inflammation and angiogenesis in AD has not been well elucidated. Prostaglandin E2 (PGE2), a key factor of the inflammatory response, has been known to promote angiogenesis. In this study, we demonstrated that PGE2 acts through EP4 receptor and protein kinase A to modulate CCAAT/enhancer-binding protein delta (CEBPD) abundance in astrocytes. Attenuated vessel formation was observed in the brains of *App*Tg/*Cebpd*$^{-/-}$ mice. We showed that miR135a was responsive to the induction of CEBPD and further negatively regulated *thrombospondin 1* (*THBS1*) transcription by directly targeting its 3′-untranslated region (3′UTR) in astrocytes. Furthermore, conditioned media from astrocytes expressing miR135a promoted Human umbilical vein endothelial cells (HUVECs) tube-like formation, which correlated with the effects of PGE2 on angiogenesis. Our results indicated that CEBPD contributes to the repression of *THBS1* transcription by activating the expression of miR135a in astrocytes following PGE2 treatment. We provided new evidence that astrocytic CEBPD increases angiogenesis during AD pathogenesis. This discovery supports the negative influence of CEBPD activation in astrocytes with respect to AD pathogenesis and implies that the CEBPD/miR135a/THBS1 axis could be a therapeutic target of AD.

1. Introduction

Neuroinflammation has been proposed to be a causative factor in the pathogenesis of Alzheimer's disease (AD), Parkinson's disease (PD), multiple sclerosis, spinal cord injury, and stroke (Czirr and Wyss-Coray, 2012; Glass et al., 2010). Prominent activation of inflammatory processes was observed in the brains of AD patients (Akiyama et al., 2000; Ikonomovic et al., 2004; Wyss-Coray, 2006). Cyclooxygenase (COX) is a microsomal enzyme that is present in 2 isoforms, COX-1 and COX-2, and is essential for the synthesis of prostaglandin E2 (PGE2), a potent inducer of inflammation. Increased levels of PGE2 and COX-2 have been observed in the cerebrospinal fluid of AD patients, and these levels also correlated with the degree of AD pathogenesis (Ho et al., 2001; Kitamura et al., 1999; Montine et al., 1999).

Inflammation is increasingly being recognized as a critical mediator of angiogenesis. A variety of studies support the hypothesis that proinflammatory cytokines and inflammatory cells may modulate angiogenesis by directly or indirectly affecting endothelial

* Corresponding author at: Institute of Bioinformatics and Biosignal Transduction, College of Bioscience and Biotechnology, National Cheng Kung University, Tainan 701, Taiwan. Tel.: +1 886 6 2757575 31067; fax: +1 886 6 2083663.
E-mail address: yumingw@mail.ncku.edu.tw (J.-M. Wang).

0197-4580/$ – see front matter © 2015 Elsevier Inc. All rights reserved.
http://dx.doi.org/10.1016/j.neurobiolaging.2014.11.020

cells, resulting in the promotion of the angiogenic process. The brains of AD patients show signs of significant hypervascularity and a high incidence of microangiopathy (Biron et al., 2011; Desai et al., 2009; Perlmutter et al., 1990). Coincident with this observation in the brains of AD patients, higher levels of vasculature have been observed in the AD mouse model (Biron et al., 2011). However, the physiological significance of this angiogenesis and its causes and mechanisms, especially the communications among the neurons, endothelia cells, and astrocytes, remain largely unknown.

We know that PGE2 plays an important role in the angiogenic process of inflammation (Leahy et al., 2000; Salcedo et al., 2003; Zhang and Daaka, 2011). Recently, a cycle of angiogenic events was suggested to contribute to Aβ accumulation and neuronal death (Vagnucci and Li, 2003). Articles also showed that the accumulating Aβ peptide in the brain parenchyma of AD patients is responsible for reduced vascular permeability (Bergamaschini et al., 2004), causing vessel disruption and loss of blood flow (Zekry et al., 2002). However, the details of PGE2-mediated signaling in astrocytes and its association with angiogenesis in AD remain unknown. The coactivation of the AMPA, kainate and metabotropic glutamate receptors on astrocytes stimulates these cells to release glutamate through a Ca^{2+}-dependent process mediated by PGE2 (Bezzi et al., 1998). PGE2 can enhance tumor necrosis factor-α (TNF-α) and interferon-γ-induced astrocytic activation by augmenting the induction of nitric oxide synthase and nitric oxide production through EP2-mediated cross talk between the cAMP/PKA and IP3/Ca^{2+} signaling pathways (Hsiao et al., 2007). However, the detailed mechanisms of PGE2 in astrocytes and its consequent effects on AD pathogenesis are still largely unknown.

CCAAT/enhancer-binding protein delta (CEBPD) belongs to the CCAAT/enhancer-binding protein (C/EBP) family and acts as a transcription factor (Ramji and Foka, 2002). CEBPD, in particular, is known to regulate or coregulate a wide range of inflammatory mediators and participate in signaling in response to interleukin-1β (IL-1β), interleukin-6 (IL-6), and TNF-α (Cardinaux et al., 2000; Ramji et al., 1993). The induction of CEBPD expression has been observed in age-associated disorders, such as neuron degeneration disease (Li et al., 2004), atherosclerosis (Yang et al., 2001), type 2 diabetes (Bennett et al., 2010), and rheumatoid arthritis (Chang et al., 2012). However, the physiological functions of CEBPD and its downstream targets in these inflammation-related diseases are poorly understood. Furthermore, IL-1β, IL-6, and TNF-α are known to be increased in the pathologic forms of neurodegenerative diseases, including AD and PD (Glass et al., 2010). CEBPD accumulates in reactive astrocytes surrounding Aβ-peptide deposits in AD (Ko et al., 2012; Li et al., 2004). In response to IL-1β, CEBPD is upregulated through the MAPK/p38 signaling pathway and is further phosphorylated by GSK3β at Ser167 in astrocytes (Ko et al., 2014). The microglia-mediated Aβ clearance by phagocytosis has been mentioned (Lee and Landreth, 2010; Simard et al., 2006), but the phagocytotic activity is reduced in AD patients (Fiala et al., 2005, 2007). The activation of astrocytic CEBPD was thought to attenuate the macrophage-mediated phagocytosis of damaged neurons and regulate the migration and activation of microglia and macrophages (Ko et al., 2012, 2014).

Thrombospondins are large, oligomeric, extracellular matrix proteins that mediate cell-cell and cell-matrix interactions by binding to other extracellular matrix proteins and an array of membrane receptors and cytokines. Studies have shown that thrombospondins participate in cell attachment, proliferation, and differentiation, as well as in apoptosis and in the inhibition of angiogenesis (Adams and Lawler, 2004; Bornstein, 2001). The expression of THBS1 in astrocytes is modulated by different secretory factors, including platelet-derived growth factor, transforming growth factor-β1, extracellular ATP, and oxygen tension (Asch et al., 1986; Scott-Drew and Ffrench-Constant, 1997; Song et al., 2002; Tran and Neary, 2006). In addition to promoting the attachment of neurons and the outgrowth of neurites (Neugebauer et al., 1991; O'Shea et al., 1991; Osterhout et al., 1992), THBS1 also critically supports astrocyte-induced synaptogenesis and neuronal migration in both normal and pathologic brain tissue, respectively (Blake et al., 2008; Christopherson et al., 2005).

MicroRNAs (miRNAs) are transcribed from the cellular genome and undergo sequential processing by several RNase complexes to produce small mature miRNAs (approximately 21–25 nt) that regulate gene expression by targeting one or more mRNAs for translational repression or cleavage (He and Hannon, 2004). The function of miRNAs intersects the RNA-mediated gene-silencing pathways at the posttranscriptional level (Yu and Kumar, 2003). By targeting the mRNAs of protein-coding genes, miRNAs play a critical role in a variety of biological processes, including development, cell growth, proliferation, and metabolism (Bueno et al., 2008). Recently, it has been suggested that the deregulation of miRNAs participates in inflammation, autoimmunity, neurodegeneration, viral infections, heart diseases, and cancer (Kanwar et al., 2010; Sonntag, 2010). To date, more than 400 miRNAs have been identified in human and chimpanzee brains (Berezikov et al., 2006; Landgraf et al., 2007). However, the functions of these miRNAs in the brain, especially in astrocytes, and how they are linked to the pathogenesis of neurodegeneration are unknown. miR135a is enriched in glial cells and has been shown to induce mitochondria-dependent apoptosis in malignant glioma (Wu et al., 2012), but the function of miR135a in inflamed brains has not been explored.

2. Methods

2.1. Materials

PGE2 was purchased from Nacalai Tesque, Inc (Kyoto, Japan). Agonists selective for each EP subtype (ONO-DI-004 for EP1, ONO-AE1-259 for EP2, ONO-AE-248 for EP3, and ONO-AE1-329 for EP4) and an EP4 selective antagonist (ONO-AE3-208) were kindly gifted by the Ono Pharmaceutical Company (Osaka, Japan). The selectivity of these compounds and the pharmacokinetics of ONO-AE3-208 have been previously reported (Kabashima et al., 2002; Narumiya and FitzGerald, 2001; Suzawa et al., 2000). The cAMP analogs (dibutyryl cAMP, N^6-Bnz-cAMP and 8-pCPT-2′-*O*-Me-cAMP), PI3 kinase inhibitor (wortmannin), PKA inhibitor (H-89), and anti-α-tubulin antibody were purchased from Sigma (St. Louis, MO, USA). An anti-Sp1 antibody was purchased from Millipore (Billerica, MA, USA). Antibodies recognizing CEBPD and THBS1 were purchased from Santa Cruz Biotechnology (Santa Cruz, CA, USA). Antibodies recognizing phospho-CREB and CREB were purchased from Cell Signaling Technology (Danvers, MA, USA). An anti-CD31 antibody was purchased from Abcam (Cambridge, UK). The TRIzol RNA extraction reagent, Lipofectamine 2000, Dulbecco's modified Eagle's medium, and Opti-MEM medium were purchased from Invitrogen (Carlsbad, CA, USA). Endothelial cell medium (ECM) was purchased from ScienCell (Carlsbad, CA, USA). The SYBR Premix ExTaq and the PrimeScript RT Reagent Kit were purchased from TaKaRa (Otsu, Shiga, Japan). All oligonucleotides were synthesized by Eurofins MWG Operon Inc (Tokyo, Japan). Fetal bovine serum was purchased from HyClone Laboratories (Logan, UT, USA).

2.2. Animals

The *App*Tg (APPswe/PS1/E9 bigenic) mice were obtained from the Jackson Laboratory (stock no. 004462, Bar Harbor, ME, USA). The *App*Tg mice were crossed with *Cebpd*$^{-/-}$ mice, a kind gift from Dr E. Sterneck (Sterneck et al., 1998) on the C57BL/6 genetic background.

Female mice heterozygous for *App*Tg mice was intercrossed with *Cebpd*$^{-/-}$ homozygous mice; the offspring (*App*Tg$^{+/-}$/*Cebpd*$^{+/-}$) were then bred to each other to produce the *App*Tg/*Cebpd*$^{-/-}$ mice in this study.

2.3. Cell culture

U373MG (human glioblastoma-astrocytoma cell line) cells were cultured in Dulbecco's modified Eagle's medium supplemented with 10% fetal bovine serum, 100 μg/mL streptomycin, and 100 units/mL penicillin. Human umbilical vein endothelial cells (HUVECs) were obtained from the Bioresource Collection and Research Center (Taiwan) and were maintained in ECM supplemented with 5% fetal bovine serum, 1% endothelial cell growth supplement, 100 μg/mL streptomycin, and 100 units/mL penicillin.

2.4. Primary astroglial preparation

The cerebral cortices were dissected in phosphate-buffered saline, carefully stripped of their meninges and digested with 0.25% trypsin in Hanks' Balanced Salt Solution (Invitrogen) for 25 minutes at 37 °C. Trypsinization was stopped by the addition of an equal volume of culture medium containing 0.02% deoxyribonuclease I (Sigma). The solution was pelleted (5 minutes, 200 g) and then resuspended into a single-cell suspension in culture medium by repeated pipetting, followed by passage through a 105-μm pore mesh. The cells were seeded on plates coated with 20 μg/mL laminin (Invitrogen). Laminin-coated plates favor astroglial growth and inhibit microglial growth (Milner and Campbell, 2002). When confluent, the cultures were treated with 10 μM cytosine arabinoside for 4 days. The cultures were used 1 day after the end of the cytosine arabinoside treatment. The vast majority of the cells were type I astrocytes, and microglia comprised less than 2% of the cells.

2.5. Quantitative real-time polymerase chain reaction

Total RNA was extracted using TRIzol according to the manufacturer's protocol and 1 μg of RNA was subjected to reverse transcription-polymerase chain reaction using the PrimeScript RT Reagent Kit. The resultant complementary DNA was mixed with the SYBR Premix ExTaq kit and appropriate primers, and quantitative polymerase chain reaction (PCR) was performed in a Thermocycler C1000 (Bio-Rad, Hercules, CA, USA). The following specific primers were used for the qRT-PCR analysis: for CEBPD, 5′-AGCGCAACAACA TCGCCGTG-3′ and 5′-GTCGGGTCTGAGGTATGGGTC-3'; for GAPDH, 5′-CCATCACCATCTTCCAGGAG-3′ and 5′-CCTGCTTCACCACCTTCTT G-3'; for THBS1, 5′-GACCTGCCACATTCAGGAGT-3′ and 5′-CTTTCTT GCAGGCTTTGGTC-3'; and for THBS1, 5′-CCAAAGCCTGCAAGAAAGA C-3′ and 5′-CCTGCTTGTTGCAAACTTGA-3'.

2.6. Microarray analysis

Total RNA was extracted using TRIzol according to the manufacturer's protocol. Samples were validated with Agilent Human and Primate miRNA OneArray (Phalanx Biotech, Taipei, Taiwan), following the manufacturers' protocols. All processes were performed by Phalanx Biotech Company. Good quality signals were obtained by filtering for scores of $p < 0.05$ in all replicates, M-value of >6 in all signals, and more than 1.5-fold change.

2.7. TaqMan reverse transcription-PCR for miRNA quantification

Total RNA was isolated using TRIzol according to the manufacturer's protocol, reverse-transcribed using the Taq-Man microRNA reverse transcription kit and subjected to real-time PCR using the TaqMan microRNA assay kit (Applied Biosystems).

2.8. Construction of plasmids

The human *CEBPD* reporter and related reporters containing site-directed mutations were described as previously mentioned (Wang et al., 2005). The fragment of 3′-untranslated region (3′UTR) of *THBS1* gene was cloned from U373MG cells by PCR with primers: THBS1-3′UTR forward, 5′-*Xba*I-TCTAGATGTAGCTTGTGCAGATGT-3′ and reverse, 5′-*Eco*RV-CTGAGATATCTATTCCAATGGCAATGAG-3'. The PCR fragment was further subcloned into pGL3-promoter vector. Mutant *THBS1 3′UTR* reporter was constructed by site-directed mutagenesis following the instructions of the QuikChang Site-directed Mutagenesis Kit (Stratagene, CA, USA) with the primer: THBS1-3′UTR mutant, 5′-AAATTGCAAAGAAAGATATCAGG TCTTCAATACT GT-3'.

2.9. Plasmid transfection and reporter gene assay

The cells were replated at an optimal density 24 hours before transfection in 6-well plastic plates. The cells were then transfected with plasmids using the FuGENE HD Transfection Reagent (Promega, Madison, WI, USA) according to the manufacturer's instructions. The total amount of DNA for each experiment was matched to their individual backbone vectors. Opti-MEM media were changed to conditioned media, and the cells were incubated for 15 hours. After transfection, the luciferase activities of the cell lysates were measured using the luciferase assay system as per the manufacturer's instructions (Promega).

2.10. Pre-miR135a and shmiR135a-inducible stable cell construction

The primers for PCR using pre-mir135a forward (5′-*Age*I-AGGCCTCGCTGTTCTCTATGGC-3′) and premir135a reverse (5′-*Pme*I-TGTCCCCGCCGTGCG-3′) to generate pre-miR135a construction in pAS4w.1.Pneo, a tetracycline inducible system of lentiviral expression vector. The shmiR135a construction in pLAS1w.3xLacO, a lentiviral expression vector, used the DNA fragment as follows: 5′-TATGGCTTTTTATTCCTATGTGACTCGAGTCACATAGGAATAAAAAG CCATATTTTT-3'. Stable U373MG cells containing Pre-miR135a and shmiR135a were generated by pLAS.AS3w.aOn.Pbsd lentiviral infectants and parental U373MG cells, respectively. Doxycycline (2 μg/mL) was used to induce miR135a expression. IPTG (500 μM) was used to induce shmiR135a expression. The lentiviral expression vectors were obtained from the National RNAi Core Facility located at the Genomic Research Center of Institute of Molecular Biology, Academia Sinica (Taiwan).

2.11. Western blot analysis

For Western blot analysis, the cells were lysed in modified RIPA buffer containing 50 mM Tris-HCl (pH 7.4), 150 mM NaCl, 1 mM EDTA, 1% Nonidet P-40, 0.25% sodium deoxycholate, 1 mM DTT, 10 mM NaF, 1 mM PMSF, 1 μg/mL aprotinin, 1 μg/mL leupeptin, and 1 mM Na_3VO_4. The lysates were resolved on a sodium dodecyl sulfate-containing 10% polyacrylamide gel, transferred to a polyvinylidene difluoride nylon membrane and probed with specific antibodies at 4 °C overnight. The levels of interested proteins were detected using a horseradish peroxidase-conjugated antibody and were revealed using an enhanced chemiluminescence Western blot system from Pierce (Rockford, IL, USA).

2.12. Lentiviral knockdown assay

Virus was produced from Phoenix cells by cotransfection of the various small hairpin RNA expression vectors in combination with pMD2.G and psPAX2. After determining the viral infection efficiency, 10 multiplicity of infection of lentivirus containing shβ-galactosidase (shLacZ) or shCEBPD were used to infect U373MG cells for 96 hours. In all lentiviral experiments, medium containing uninfected viruses was removed before conducting further assays. The small hairpin RNA sequences in lentiviral expression vectors were: shβ-galactosidase: 5′-CCGGTGTTCGCATTATCCGAACCATCT CGAGATGGTTCGGATAATGCGAACATTTTTG-3′, shCEBPD (shC7): 5′-CCGGGCTGTCGGCTGAGAACGAGAACTCGAGTTCTCGTTCTCAGCCGACA GCTTTTT-3′ and shCebpd (shE4) 5′-CCGGCAGCGCCTACATTGACTCCA TCTCGAGATGGAGTCAATGTAGGCGCTGTTTTTG-3′. The lentiviral knockdown expression vectors were obtained from the National RNAi Core Facility located at the Genomic Research Center of Institute of Molecular Biology, Academia Sinica (Taiwan).

2.13. Chromatin immunoprecipitation assay

The chromatin immunoprecipitation assay was performed essentially as described by Wang et al. (2006). Briefly, U373MG cells were treated with 1% formaldehyde at room temperature. The cross-linked chromatin was then sonicated to an average size of 500 bp. The chromatin fragments were then immunoprecipitated with antibodies specific for Sp1, CREB, or control rabbit immunoglobulin G at 4 °C overnight. After the cross-linking was reversed, the immunoprecipitated chromatin was amplified using primers targeting specific regions of the target genomic loci. The following primers were used: 5′-CGAGGAGGTTCCAAGCCCAC-3′ and 5′-GGCTGTCACCTCGCTGGG CC-3′. The amplified DNA products were resolved by agarose gel electrophoresis and confirmed by sequencing.

2.14. In vitro capillary tube-like formation assay

Forty-eight well plated were precoated with Matrigel (BD Biosciences, Mountain View, CA, USA), which was allowed to solidify for 1 hour at 37 °C. HUVEC endothelial cells were (3×10^4 cells/well) suspended in ECM medium or combined with different conditional media and were added to each well. After 6 hours incubation, phase-contrast images of HUVECs seeded on Matrigel were captured by using an inverted light microscope (LEICA CTR 4000, Switzerland) at ×10 magnification. Images were analyzed and quantified by using image analysis services provided by Wimasis (Munich, Germany).

2.15. Immunohistochemistry

Male mouse brain tissue dissections from *App*Tg or *App*Tg/*Cebpd*$^{-/-}$ mice (approximately 15–16 months of age) were post-fixed in 4% buffered paraformaldehyde for 24–36 hours, cryoprotected, and sectioned at 10 μm on a freezing microtome. The frozen sections were treated with protein blocker and/or antibody diluents (Bio SB, Santa Barbara, CA, USA) for 1 hour. In the same buffer solution, the sections were incubated overnight with anti-CD31 antibody at 4 °C. After incubation, the sections were washed in PBS and incubated in the ABC kit solutions (Vector Laboratories, Burlingame, CA, USA) for 1.5 hours. The sections were stained with diaminobenzidine (Sigma) and mounted on slides and sealed with coverslips. The images were observed with phase contrast on BX51 microscope (Olympus, Tokyo, Japan) with a 40× objective and using DP70 digital camera system combined with DP Controller software (Ver. 2.2.1.195, Olympus). Vessels were counted in 4 acquired nonoverlapping images per slice section of each animal. For the quantification of microvessels, the longitudinal vessel segment between the 2 nodes (join points) was considered as a vessel unit. All quantifications were performed by an observer blinded to the experimental condition of each animal.

2.16. Statistical analysis

The data were analyzed by 1-tailed unpaired Student *t* test for 2 groups of experiment using Prism 5 software. For 3 or more groups of experiment, the data were analyzed by 1-way analysis of variance followed by the Bonferroni multiple comparison test using Prism 5 software. A probability of $p < 0.05$ was considered significant in all comparisons.

3. Results

3.1. PGE2 activates CEBPD expression through the EP4 receptor in astrocytes

The production of PGE2 in astrocytes contributes to astrocyte activation in inflamed brains (Bezzi et al., 1998; Font-Nieves et al., 2012; Xu et al., 2003). Recently, it was reported that PGE2 activates CEBPD in macrophages (Hsiao et al., 2013). We found that PGE2 also activated CEBPD in astrocytes (Fig. 1A). Four PGE2 receptors have been identified in astrocytes (Fiebich et al., 2001; Waschbisch et al., 2006). To assess which receptor plays a potent role in the PGE2-induced CEBPD activation in astrocytes, 4 selective agonists of each EP subtype (ONO-DI-004 [DI-004] for EP1, ONO-AE1-259 [AE1-259] for EP2, ONO-AE-248 [AE-248] for EP3, and ONO-AE1-329 [AE1-329] for EP4) were used to treat U373MG cells. AE1-329 could efficiently induce *CEBPD* transcription (Fig. 1B). Meanwhile, in addition to the response of *CEBPD* transcription to PGE2 treatment, the expression of CEBPD was induced by PGE2 and AE1-329 (Fig. 1C). In agreement with the effect of AE1-329 on *CEBPD* transcription, the EP4 selective antagonist, ONO-AE3-208 (AE3-208), showed an inhibitory effect on the PGE2-and AE1-329-induced *CEBPD* transcription in a dose-dependent manner (Fig. 1D and E).

3.2. Role of the PKA signaling pathway in PGE2-induced CEBPD transcription

Both the PI3 kinase (PI3K) and PKA pathways have been reported to play important roles in PGE2-EP4 signaling (Hirata and Narumiya, 2011). We further determined which signaling pathway(s) was involved in the PGE2/EP4-induced *CEBPD* transcription, and the PKA inhibitor H89 and the PI3K inhibitor wortmannin were used to reveal the involvement of PKA and/or PI3K in astrocytes. A coincident result showed that H89, but not wortmannin, attenuated the PGE2-and AE1-329-induced *CEBPD* transcripts (Fig. 2A). Furthermore, various cAMP analogs, including the 2 specific PKA activators dibutyryl cAMP (db-cAMP) and N^6-Bnz-cAMP and the exchange proteins activated by cAMP (Epac) activator 8-pCPT-2′-O-Me-cAMP, were used to verify the involvement of PKA in the activation of CEBPD transcription in astrocytes. Similar to PGE2 action, the 2 specific PKA activators, db-cAMP and N^6-Bnz-cAMP, showed a coincident effect in the activation of CEBPD transcripts (Fig. 2B). These results suggested that PKA, at least in part, mediated the PGE2-induced *CEBPD* transcription.

3.3. Involvement of CREB and Sp1 in the PGE2-induced CEBPD gene transcription

The proximal region near the transcription initiation site of the *CEBPD* promoter, which contains 2 Sp1 motifs and 1 CRE motif, is important for *CEBPD* transcriptional activation (Wang et al., 2005).

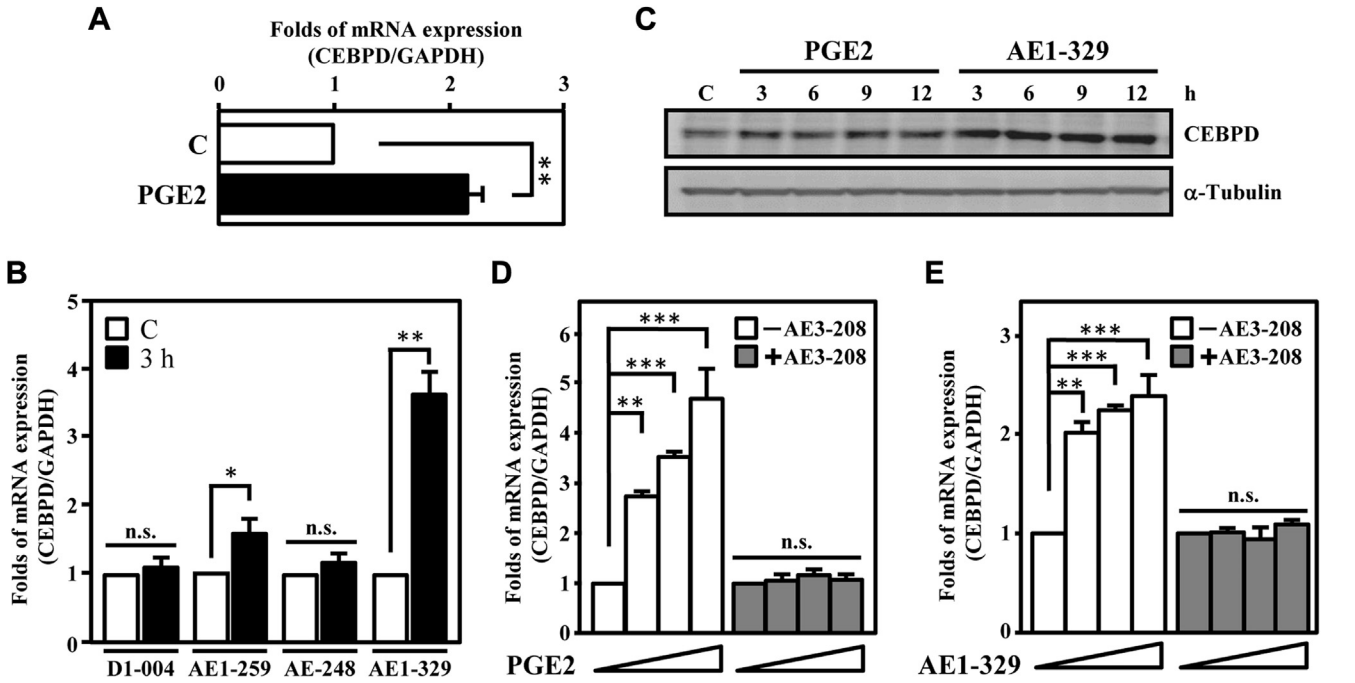

Fig. 1. The EP4 receptor mediates the PGE2-induced CEBPD expression in U373MG cells. (A) U373MG cells were treated with 50 μM PGE2 for 3 hours, and total RNA was harvested. qRT-PCR analysis was conducted to examine the expression of *CEBPD* mRNA (mean ± standard error, $^{**}p < 0.01$, Student *t* test). (B) U373MG cells were individually treated with selective agonists of the EP subtypes (5 μM of DI-004 for EP1, 0.5 μM of AE1-259 for EP2, 1 μM of AE-248 for EP3, and 1 μM of AE1-329 for EP4). Total RNA was harvested from the experimental cells at the indicated time points. qRT-PCR analysis was conducted to examine the expression of *CEBPD* mRNA. (C) U373MG cells were treated with 50 nM PGE2 or 1 μM EP4 agonist. At the indicated time points, cell lysates were harvested for Western blot analysis using anti-CEBPD or anti-α-tubulin antibodies. (D) The EP4 selective antagonist (AE3-208) attenuated the level of *CEBPD* mRNA following PGE2 treatment. U373MG cells were treated with the indicated chemicals. The cells were treated with PGE2 and AE3-208 (D) or AE1-329 and AE3-208 (E) for 3 hours. The level of *CEBPD* mRNA was examined using qRT-PCR analysis. (B, D, and E) ANOVA (mean ± standard error, $^{*}p < 0.05$, $^{**}p < 0.01$, $^{***}p < 0.001$, n = 3 per group). Abbreviations: ANOVA, analysis of variance; C, control; CEBPD, CCAAT/enhancer-binding protein delta; mRNA, messenger RNA; n.s., not significant; PGE2, prostaglandin E2; qRT-PCR, quantitative real-time polymerase chain reaction.

It is known that the cAMP signaling pathway activates CREB through PKA (Delghandi et al., 2005; Hirata and Narumiya, 2011). Treatment with PGE2 or AE1-329 resulted in the phosphorylation of CREB Ser133 in U373MG cells (Fig. 3A). A dominant negative mutant of CREB (DN-CREB), in which the serine 133 residue was mutated to alanine, was used to assess whether CREB participated in the PGE2-induced *CEBPD* transcription. The result showed that DN-CREB inhibited both the PGE2-and AE1-329-induced *CEBPD* reporter activity (Fig. 3B). Additionally, a decrease in Sp1 also repressed the PGE2-and AE1-329-activated *CEBPD* reporter activity (Fig. 3C). The overexpressed CREB-induced *CEBPD* reporter activity was attenuated in the *CEBPD* reporter that contained a mutated

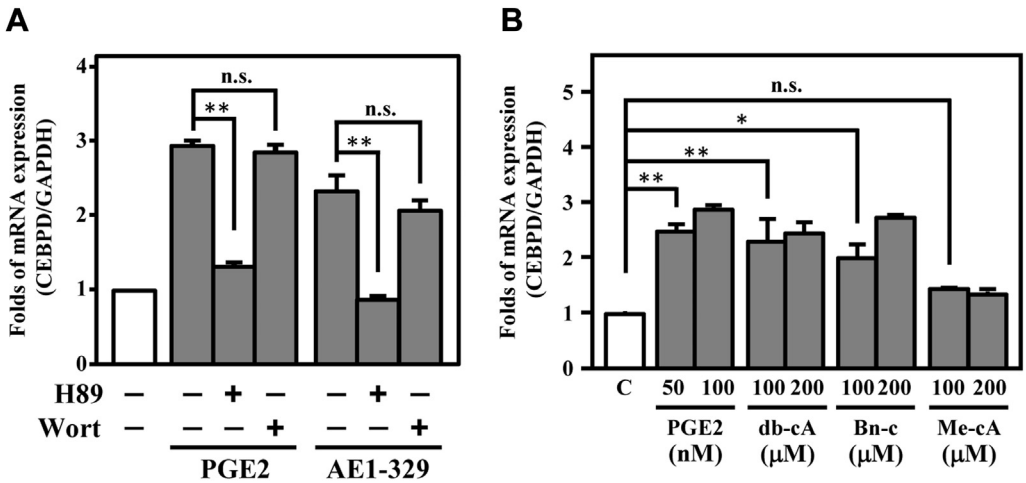

Fig. 2. The PKA signaling pathway participates in PGE2-induced CEBPD expression. (A) H89 attenuates the PGE2-induced *CEBPD* transcription. U373MG cells were pretreated with inhibitors of PKA (H89, 10 μM) or PI3K (wortmannin [Wort], 0.1 μM) before being re-stimulated with PGE2 or AE1-329 for 3 hours. qRT-PCR analysis was performed to examine the expression of *CEBPD* mRNA. (B) The effects of cAMP analogs on *CEBPD* mRNA expression. U373MG cells were treated with PGE2 or various cAMP analogs for 3 hours. qRT-PCR analysis was conducted to amplify the indicated genes with specific primers. ANOVA (mean ± standard error, $^{*}p < 0.05$, $^{**}p < 0.01$, n = 3 per group). Abbreviations: ANOVA, analysis of variance; Bn-c, N^6-Bnz-cAMP; db-cA, db-cAMP; Me-cA, 8-pCPT-2′-*O*-Me-cAMP; CEBPD, CCAAT/enhancer-binding protein delta; mRNA, messenger RNA; n.s., not significant; PGE2, prostaglandin E2; qRT-PCR, quantitative real-time polymerase chain reaction.

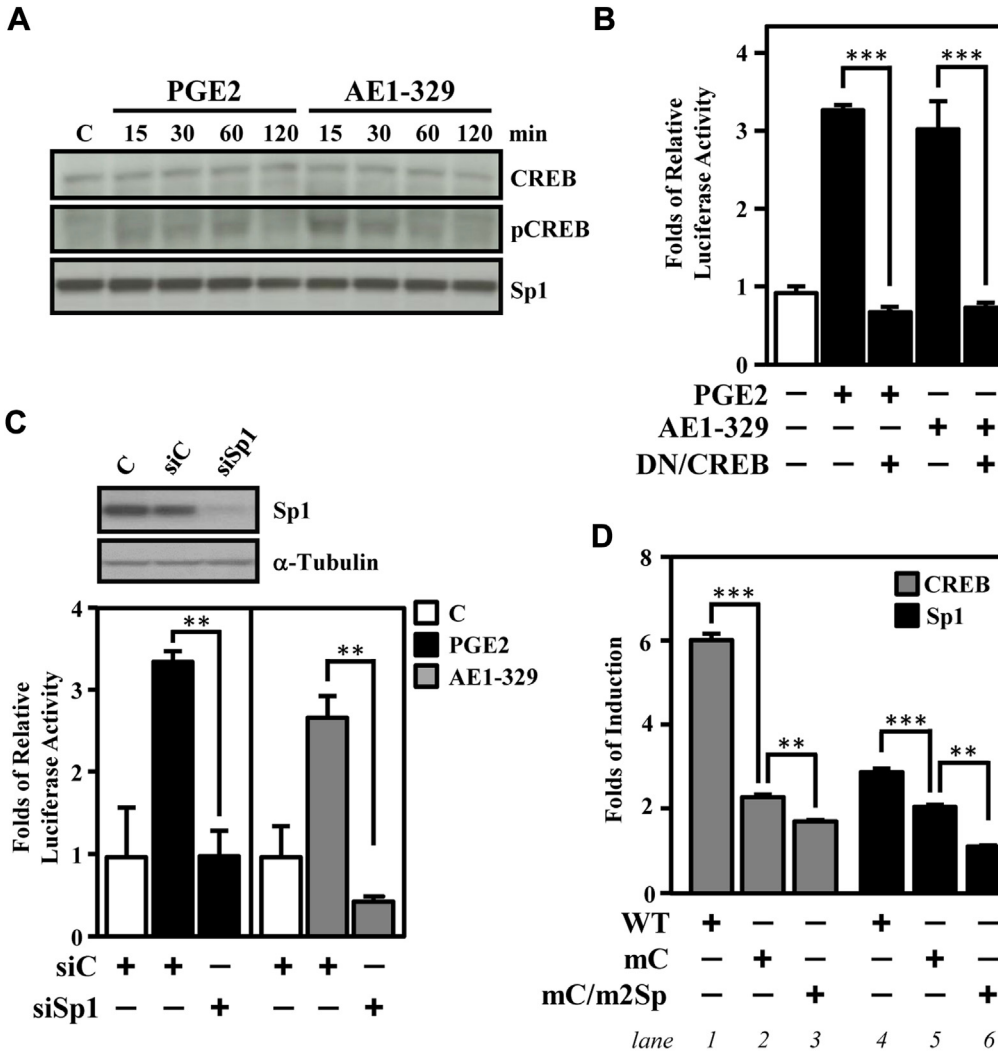

Fig. 3. CREB and Sp1 participate in PGE2-induced CEBPD transcription. (A) CREB protein is activated on PGE2 treatment in U373MG cells. U373MG cells were treated with PGE2 or AE1-329. At the indicated time points, cell lysates were harvested and Western blot analysis was performed using anti-CREB, anti-phospho-CREB (Ser133), or anti-Sp1 antibodies. (B) U373MG cells were transiently transfected with the CEBPD reporter (CEBPD −348/+9), pcDNA3 or pcDNA3/CREBS133A (DN-CREB) expression vectors. After transfection, the cells were treated with PGE2 or AE1-329 for 3 hours. Lysates were prepared from the experimental cells and were used for the luciferase assay. (C) Loss of Sp1 attenuates the PGE2-induced CEBPD reporter activity. U373MG cells were transfected with si-control (siC) or siSp1 for 12 hours and then transfected with CEBPD reporter. After 6 hours, the cells were treated with PGE2 or AE1-329 for 3 hours. The lysates were then harvested from the experimental cells for the luciferase assay. (D) Both Sp1 and CRE motifs are important for the PGE2-induced CEBPD reporter activity. U373MG cells were transfected with the reporters or expression vectors as indicated. After 16 hours, cell lysates were harvested for

CREB binding motif (mC) and further reduction was observed in the *CEBPD* reporters that contained mutated Sp1 and CREB binding motifs (mC/m2Sp) (Fig. 3D, compare lanes 2 and 3 with lane 1). Meanwhile, the transfectants that overexpressed Sp1 showed a reduced *CEBPD* reporter activity when the CREB binding motif was mutated, and this activity was further reduced when both the Sp1 and CREB binding motifs were mutated (Fig. 3D, compare lanes 5 and 6 with lane 4). We next conducted an in vivo DNA binding assay to assess the direct binding of CREB and Sp1 to the promoter of the *CEBPD* gene. The PCR results of the ChIP assay showed that CREB and Sp1 were responsive to PGE2 or AE1-329 and these factors directly bound the promoter of the *CEBPD* gene (Fig. 3E). Furthermore, to assess whether CREB and Sp1 formed a complex that could bind to the promoter of the *CEBPD* gene, a re-ChIP assay was performed. The PCR results of the re-ChIP assay showed that the interaction between CREB and Sp1 was responsive to PGE2 treatment, and these factors could form a complex to bind to the promoter of the *CEBPD* gene (Fig. 3F). These results indicated that Sp1 and CREB could directly and cooperatively participate in the PGE2-induced *CEBPD* transcriptional activation in astrocytes.

3.4. PGE2 negatively regulates THBS1 expression through CEBPD in astrocytes

As mentioned previously, PGE2 exerts a proangiogenic effect through the activation of the EP4 receptor (Zhang and Daaka, 2011). Compared with the *App*Tg mice, the angiogenic effect was attenuated in the *App*Tg/*Cebpd*$^{-/-}$ mice (Fig. 4A). CEBPD is highly expressed in astrocytes surrounding Aβ plaques in AD patients and *App*Tg mice (Ko et al., 2012, 2014). We further tested whether astrocytic CEBPD plays a functional role in the PGE2-induced angiogenesis. The conditioned media from PGE2-treated or CEBPD-overexpressed astrocytes could promote the tube-like formation of HUVECs (Fig. 4B). Moreover, the attenuation of CEBPD could reduce the PGE2-promoted tube-like formation effect (Fig. 4C and Supplementary Fig. 3A). These results implied that the gain of secretory angiogenic inducer(s) or the loss of angiogenic suppressor(s) was responsive to the activation of CEBPD and the treatment of PGE2 in astrocytes.

THBS1 plays an anti-angiogenic role and was downregulated in the CEBPD-overexpressed astrocytes (Ko et al., 2012). The levels of *THBS1* messenger RNA (mRNA) and protein were repressed in U373MG cells on PGE2 treatment (Fig. 4D). Similar to the U373MG cells (Fig. 4E, left panel, compare lane 4 with lane 2), the attenuation of CEBPD could restore the PGE2-repressed THBS1 expression in mouse primary astrocytes (Fig. 4E, right panel). These results suggested that CEBPD participates in the PGE2-repressed *THBS1* transcription in astrocytes. As mentioned previously, miRNA contributes to transcriptional repression by binding to the 3′UTRs of target genes. To determine whether a miRNA contributes to the CEBPD-repressed *THBS1* transcription, a miRNA microarray was conducted using total RNA from stable U373MG cells expressing $ZnSO_4$-inducible CEBPD. The miR135a, a potent *THBS1* mRNA binding suppressor, was identified and upregulated by CEBPD. PGE2 could induce the abundance of miR135a in U373MG cells (Fig. 5A). Furthermore, the luciferase activity of the *THBS1 3′UTR* reporter, which contained a miR135a targeting motif, was suppressed on PGE2 treatment. In contrast, this repression was lost in the *THBS1 3′UTR* reporter that contained a mutant miR135a targeting motif (Fig. 5B). Moreover, treatment with miR135a inhibitor (AM135a) could reverse the effect of PGE2-repressed expression of *THBS1* mRNA and protein in U373MG cells (Fig. 5C).

3.5. Angiogenic effect observed in the conditioned medium from astrocytes expressing miR-135a

As shown previously, the conditioned media of the PGE2-treated and CEBPD-overexpressed U373MG cells contributed to the tube-like formation of HUVECs. THBS1 has been suggested to serve as an angiogenic suppressor. We demonstrated that the CEBPD-induced miR135a can bind to the 3′UTR of *THBS1* mRNA, which resulted in decreased levels of THBS1 in the CEBPD-overexpressed or PGE2-treated conditioned medium. To assess the potential role of miR135a in the regulation of angiogenesis, 2 stable U373MG clones expressing inducible miR135a were established. The conditioned media from the 2 miR135a-expressed U373MG cell lines promoted the tube-like formation of HUVECs (Fig. 6A). Moreover, a reversed effect was observed in the HUVECs or bEnd.3 cells cultured in the conditioned medium from U373MG/miR135a-1 cells transfected with the miR135a inhibitor (Fig. 6B and Supplementary Fig. 3B).

4. Discussion

In this study, we demonstrated that CEBPD negatively regulates *THBS1* transcription by increasing the expression of miR135a after PGE2 treatment in astrocytes. The miR135a contributed to the repression of *THBS1* transcription by targeting the *THBS1* 3′UTR. Furthermore, conditioned media from astrocytes expressing miR135a inhibited the tube-like formation of HUVECs. This discovery supports the negative influence of elevated CEBPD with respect to AD pathogenesis and provides evidence that the CEBPD/miR135a/THBS1 axis could be a therapeutic target for AD.

PGE2 can induce *CEBPD* transcription in macrophages through the posttranscriptional regulation of RNA-binding protein Hu antigen R (HuR)-stabilized CEBPD mRNA (Hsiao et al., 2013). Interestingly, the contribution of CEBPD promoter-mediated transcriptional activation is limited in response to PGE2 in macrophages. Contrary to what is observed in macrophages, PGE2 and the EP4 agonist AE1-329 had no effect on the stabilization of *CEBPD* mRNA in U373MG cells (Supplementary Fig. 1). These results suggested that the PGE2-mediated regulation of CEBPD occurs in a cell type- or tissue-specific manner. PGE2 interacts with different G protein-coupled EP receptors to initiate multiple intracellular signaling cascades, leading to the induction of inflammatory response (Hirata and Narumiya, 2011). Nonsteroidal anti-inflammatory drugs (NSAIDs), which inhibit COX, can delay the onset and reduce the risk of AD (in ‘t Veld et al., 2001; McGeer et al., 1990). However, the administration of NSAIDs to AD patients raises the concern of off-target effects because of the complexity and reciprocal regulation of the EP receptors; therefore, NSAID administration may also result in insufficient treatment (Imbimbo et al., 2010; in ‘t Veld et al., 2001) (Hoozemans and O’banion, 2005).

luciferase assay. (E, F) CREB and Sp1 bind to the *CEBPD* promoter. Sheared formaldehyde cross-linked chromatin was immunoprecipitated with the indicated antibodies and processed for PCR amplification. As a positive control, PCR amplification was also performed with input chromatin that was collected before the immunoprecipitation step (lanes 1, 2, and 3). The chromatin was isolated from cells treated with or without PGE2 and AE1-329. An immunoprecipitation (IP) step was performed with the indicated antibodies (IP Abs). “−348/+9” indicates the PCR products after amplification with specific primers using purified templates from the specific antibody-IP step. ANOVA (mean ± standard error, $^{**}p < 0.01$, $^{***}p < 0.001$, n = 3 per group). Abbreviations: ANOVA, analysis of variance; CEBPD, CCAAT/enhancer-binding protein delta; mC, CEBPD reporter CREB site mutated; mC/m2Sp, CEBPD reporter CREB site and 2 Sp1 sites mutated; PCR, polymerase chain reaction; PGE2, prostaglandin E2; WT, CEBPD reporter (CEBPD −348/+9). (For interpretation of the references to color in this Figure, the reader is referred to the Web version of this article.)

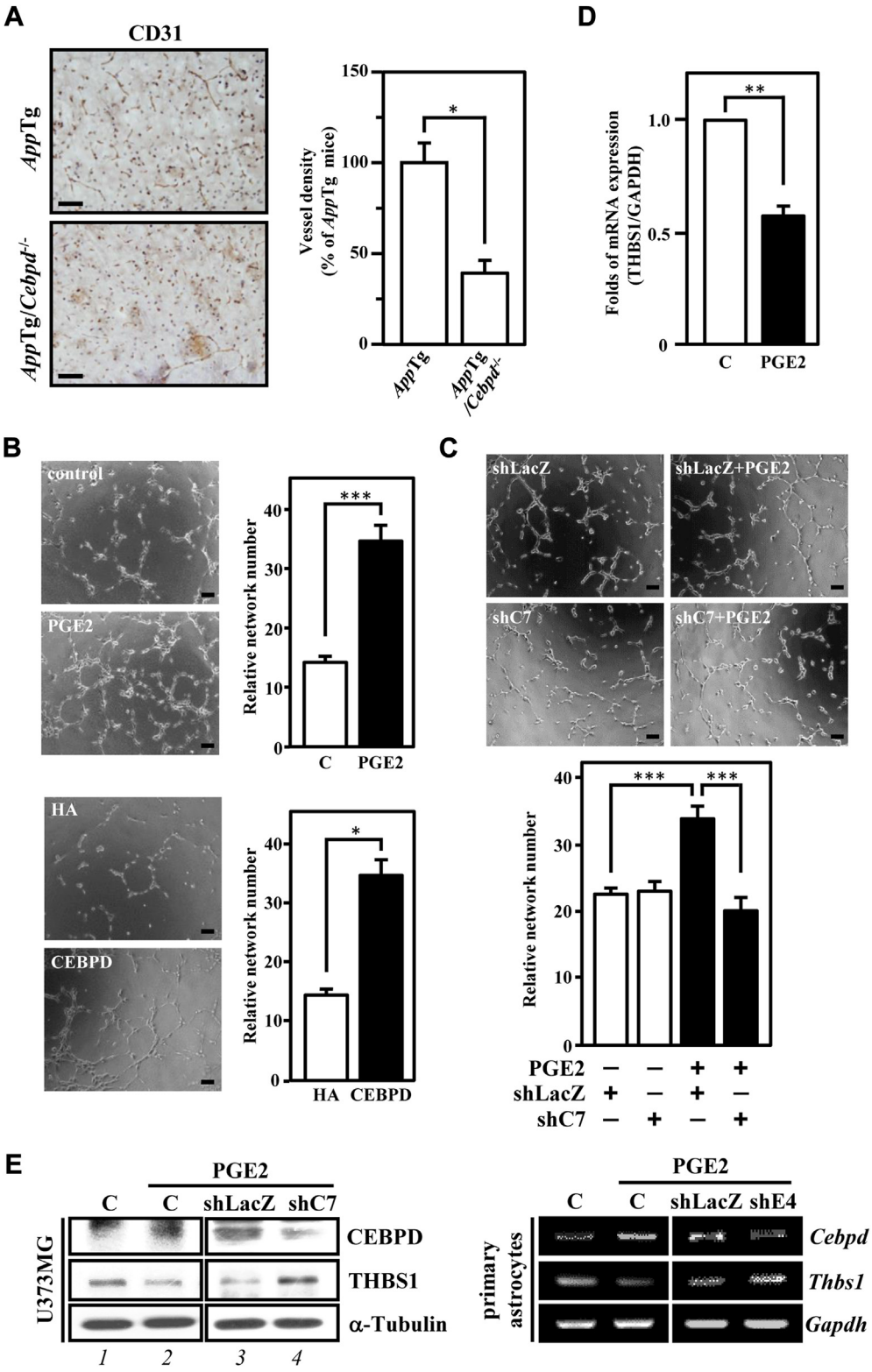

Fig. 4. PGE2 negatively regulates THBS1 expression through CEBPD in astrocytes. (A) Loss of CEBPD attenuated the angiogenic effect in *App*Tg/*Cebpd*$^{-/-}$ mice. Sagittal sections of brain cortex were prepared from *App*Tg or *App*Tg/*Cebpd*$^{-/-}$ mice and were subjected to immunohistochemistry with an anti-CD31 antibody. Representative images (left) and quantification of vessel density (right) on 15–16 months aged mice. Scale bar = 50 μm. (B) HUVECs were plated on a Matrigel-coated plate containing conditioned media from PGE2-treated or CEBPD-overexpressed U373MG cells. Scale bar = 100 μm. (C) HUVECs were plated on a Matrigel-coated plate containing indicated conditioned media. Scale bar = 100 μm. (D) U373MG cells were treated with PGE2 for 3 hours, and *THBS1* mRNA expression was then examined using qRT-PCR. (E) Loss of CEBPD reverses the PGE2-attenuated THBS1 expression. U373MG cells (left panel) or primary astrocytes (right panel) were transfected with shβ-galactosidase (shLacZ), shCEBPD (shC7), or shCebpd (shE4) and then treated with PGE2 for 3 hours. Total RNA or cell lysates were harvested for qRT-PCR or Western blot analysis. (A, B, and D) (mean ± standard error, $^{*}p < 0.05$, $^{**}p < 0.01$, $^{***}p < 0.001$, Student *t* test); (C) ANOVA analysis (mean ± standard error, $^{***}p < 0.001$, n = 6 per group). Abbreviations: ANOVA, analysis of variance; CEBPD, CCAAT/enhancer-binding protein delta; HUVECs, Human umbilical vein endothelial cells; mRNA, messenger RNA; PGE2, prostaglandin E2; qRT-PCR, quantitative real-time polymerase chain reaction; THBS1, thrombospondin 1. (For interpretation of the references to color in this Figure, the reader is referred to the Web version of this article.)

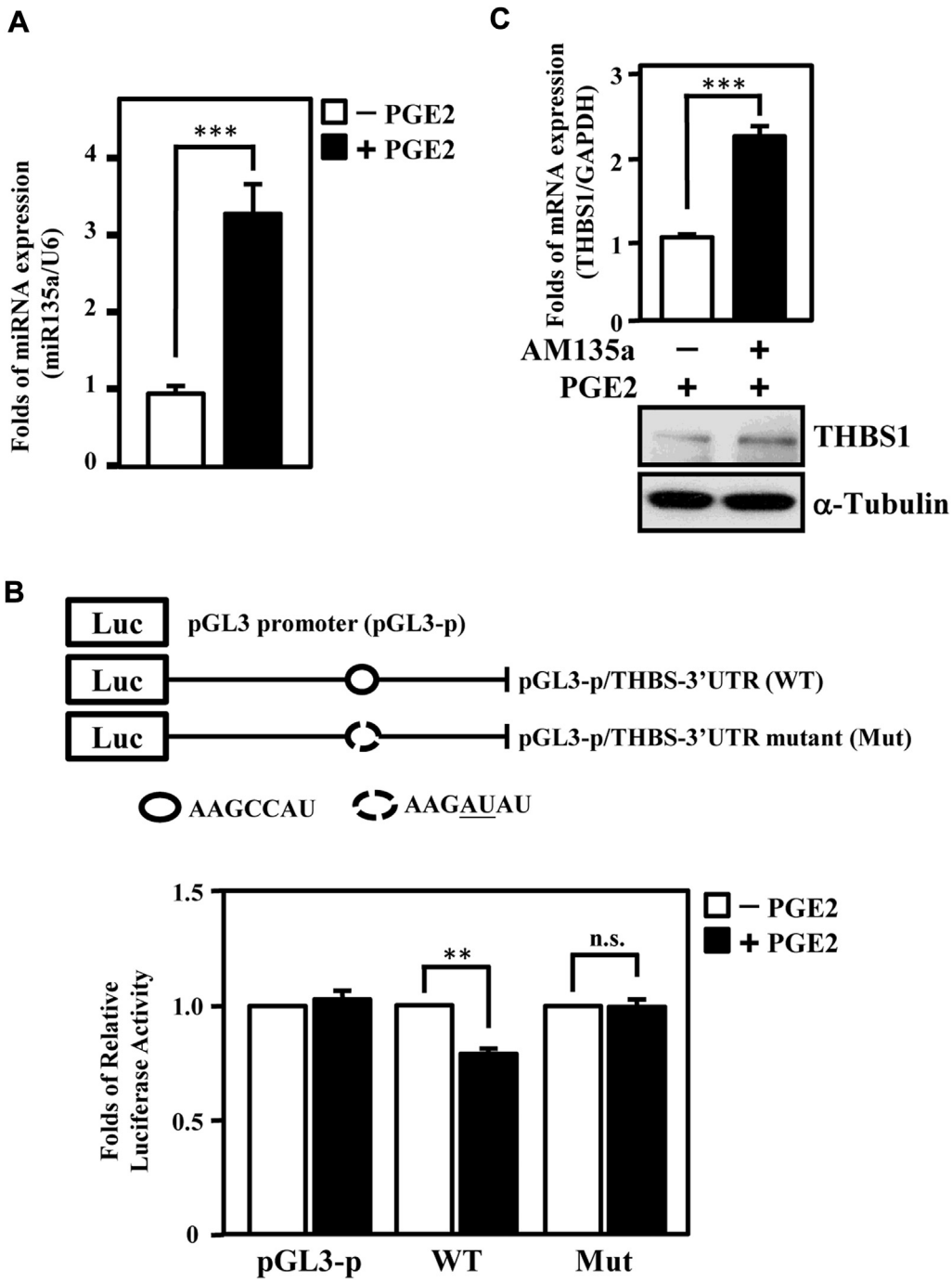

Fig. 5. miR135a mediates the PGE2-repressed *THBS1* transcription through its 3′UTR region. (A) The level of miR135a is upregulated following PGE2 treatment. U373MG cells were treated with PGE2 for 3 hours, and miR135a expression was examined using qRT-PCR analysis. (B) The miR135a target site in the *THBS1* 3′UTR is important for *THBS1* suppression following PGE2 treatment. The putative miR135a binding site in the *THBS1* 3′UTR was predicted using the TargetScan program (upper panel). The seed region is indicated by the open circle. The reporters with or without the *THBS1* 3′UTR were transfected into U373MG cells after PGE2 treatment. The experimental lysates were prepared and used for the luciferase assay. (C) U373MG cells were transfected with miR135a inhibitor (AM135a) and then treated with PGE2 for 3 hours. qRT-PCR and Western blot analyses were performed to examine the expression of THBS1 mRNA and protein. (A and C) Mean ± standard error, *** $p < 0.001$, Student's t test; (B) ANOVA (mean ± standard error, ** $p < 0.01$, n = 3 per group). Abbreviations: 3′UTR, 3′-untranslated region; ANOVA, analysis of variance; PGE2, prostaglandin E2; qRT-PCR, quantitative real-time polymerase chain reaction; THBS1, thrombospondin 1.

The levels of EP2 and EP4 receptors are higher than the levels of EP1 and EP3 receptors in U373MG cells, and EP4 is thought to contribute to PGE2-induced IL-6 release (Fiebich et al., 2001). Using agonists for the various EP receptors, the EP4 agonist AE1-329 showed the most dominant effect on *CEBPD* mRNA activation. Meanwhile, the EP4 antagonist AE3-208 significantly abolished the PGE2-induced *CEBPD* transcription. A study showed that the oral administration of AE3-208 to AD mice (APP23) improved their cognitive performance and suppressed the Aβ-mediated activation of astrocytes (Hoshino et al., 2012). These discoveries suggested that EP4 could play a crucial role in the pathogenesis of AD and could be a more specific target for AD therapy.

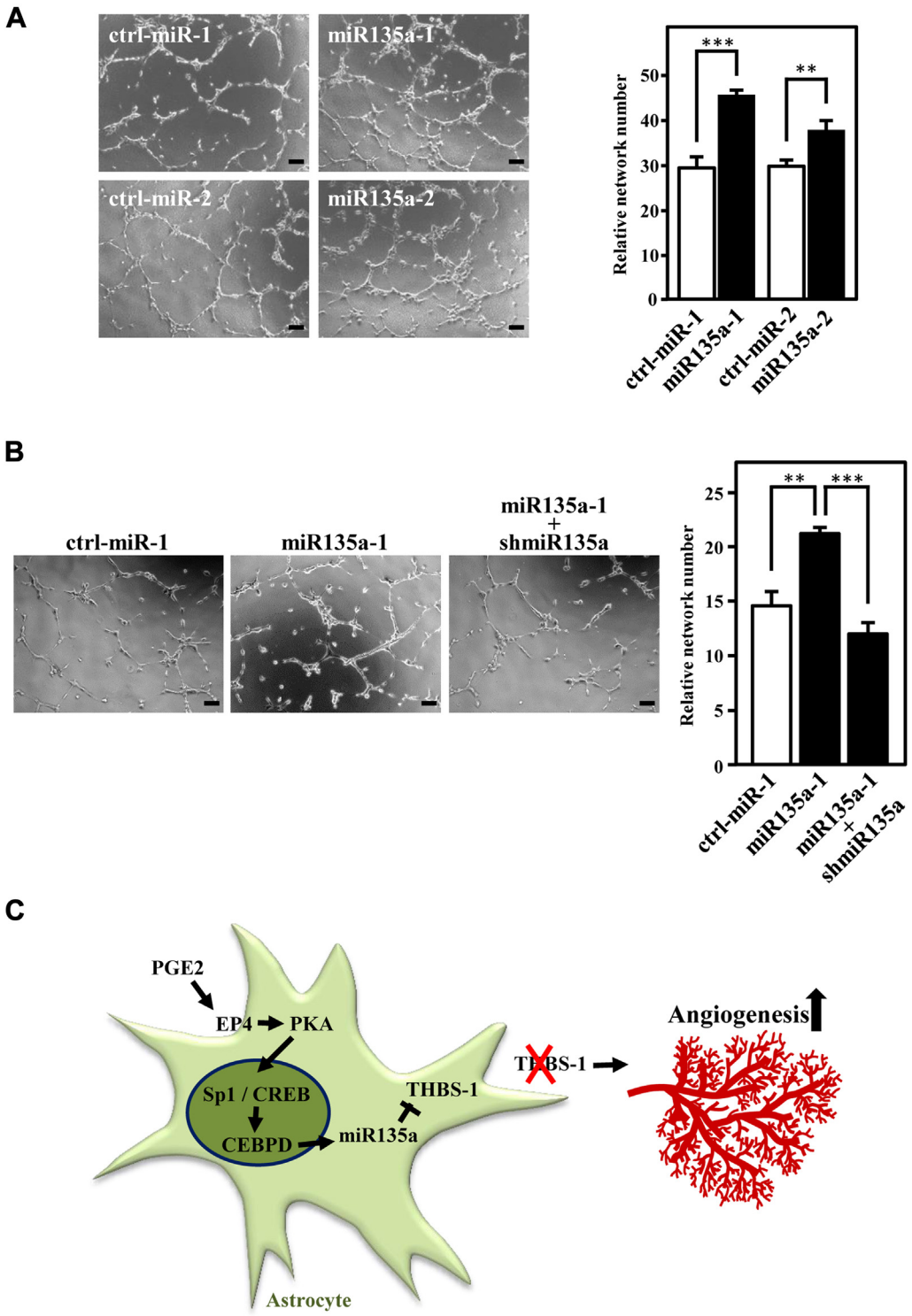

Fig. 6. miR135a exhibits an angiogenic effect. (A and B) HUVECs were plated on a Matrigel-coated plate and grown in conditioned media from PGE2-treated U373MG cells, various miR-135a stable clones or combined shmiR135a in U373MG cells. (C) A proposed model for astrocytic CEBPD-mediated angiogenesis in Alzheimer's disease. In astrocytes, PGE2 acts through EP4 receptor and PKA to activate CEBPD. The miR135a is responsive to the induction of CEBPD and further targeting to *THBS1* 3′UTR. The repression of *THBS1* transcripts reduces THBS1 releasing from astrocytes and therefore promotes angiogenesis. ANOVA (mean ± standard error, $^{**}p < 0.01$, $^{***}p < 0.001$, n = 6 per group). Scale bar = 100 μm. Abbreviations: 3′UTR, 3′-untranslated region; ANOVA, analysis of variance; CEBPD, CCAAT/enhancer-binding protein delta; Ctrl, control; HUVECs, Human umbilical vein endothelial cells; PGE2, prostaglandin E2; PKA, protein kinase A; THBS1, thrombospondin 1. (For interpretation of the references to color in this Figure, the reader is referred to the Web version of this article.)

Most effects of PGE2 have been attributed to its stimulation of cAMP formation via the EP2 or EP4 receptors (Hirata and Narumiya, 2011). In agreement with the result that the PKA inhibitor H89 suppressed EP4-induced CEBPD activation, loss of function assays showed that db-cAMP and its analog N^6-Bnz-cAMP, but not 8-pCPT-2′-*O*-Me-cAMP, could also induce the expression of CEBPD in U373MG cells. The results suggested that the induction of CEBPD in astrocytes is in response to the canonical PGE2-EP4-cAMP-PKA

signaling pathway. Additionally, we also found that PGE2 and AE1-329 can activate MAPK/p38 in U373MG cells (Supplementary Fig. 2). MAPK/p38 can be activated via a cAMP-dependent or cAMP-independent pathway (Delghandi et al., 2005; Fiebich et al., 2001). On Epidermal growth factor, IL-1β or TNF-α treatments, MAPK/p38 plays an important role in the activation of *CEBPD* transcription (Ko et al., 2012; Wang et al., 2005). Therefore, the involvement of MAPK/p38 in PGE2-induced *CEBPD* transcription remains to be further clarified.

It is thought that the deregulation of miRNAs may participate in the pathogenesis of neurodegeneration. However, the whole picture and the detailed mechanisms remain largely unknown, especially in astrocytes and their associated diseases. The associations of several miRNAs with AD, Huntington disease, PD, neuroviral infections, and schizophrenia have been identified (Lau and de Strooper, 2010; Thounaojam et al., 2013). Previously, the upregulation of miR135a was shown in a microarray profile of brain tissues from AD mice (Lee et al., 2012), but how it is regulated and its involvement in AD pathogenesis remain unknown. The known miR135a-targeted genes, *STAT6*, *SMAD5*, and *BMPR2*, were suggested to induce angiogenesis in the other tissues (de Jesus Perez et al., 2009; Nishimura et al., 2008; Yamaji-Kegan et al., 2009; Yang et al., 1999), but their roles in astrocytes and inflamed brains are unclear. The c-Myc-induced miR-17-92 miRNA cluster and the KSHV-encoded miRNA-K12 cluster have been suggested to contribute to neovascularization by downregulating THBS1 (Dews et al., 2006; Samols et al., 2007). The brains of AD patients exhibited decreased THBS1 staining (Buee et al., 1992) and Aβ inhibits the release of THBS1 from astrocytes and contributes to the loss of synaptophysin in neurons (Rama Rao et al., 2013). Herein, in agreement with the loss of THBS1 in the brains of AD patients, we provided new insight into the role of miR135a in angiogenesis during AD pathogenesis through the suppression of the THBS1 gene.

Although the observation that the upregulation of angiogenic mediators such as vascular endothelial growth factor (VEGF) has been demonstrated in AD pathogenesis, the reduction and detailed mechanism of inhibition of angiogenic suppressors remain largely uncharacterized. Epidemiologic studies have shown that long-term use of anti-inflammatory drugs, statins, or calcium-channel blockers could prevent AD (Forette et al., 1998; in 't Veld et al., 2001; Jick et al., 2000). Importantly, these drugs also have been suggested to play functional role in inhibition of angiogenesis (Jesmin et al., 2002; Jones et al., 1999). Therefore, further identification of the novel targets and development of antiangiogenic drugs targeting the abnormal brain endothelial cell might be able to prevent and treat this disease. However, a recent study showed that VEGF can recover vascular abnormalities and cognitive. It also recovers social behavioral deficits in VEGF-transplanted AD model mice (Garcia et al., 2014). The result not only indicates that the dissection of details in angiogenesis of AD pathogenesis is necessary and also implies that the administration of drugs targeting angiogenesis in AD patients needs a further evaluation.

Angiogenic vessels are often surrounded by inflammatory microglia and macrophages, suggesting that activated microglia and/or macrophages may be instrumental in promoting the angiogenic response to cerebral inflammation (Jander et al., 1998; Jantaratnotai et al., 2010; Manoonkitiwongsa et al., 2001). Additionally, conditioned media taken from activated microglia and macrophages directly promoted endothelial cell proliferation in vitro (Polverini et al., 1977; Welser et al., 2010). Recently, we found that astrocytic CEBPD plays an important role in the activation of microglia and/or macrophages (Ko et al., 2014). Thus, elevated CEBPD expression in astrocytes could contribute to the angiogenesis of brain endothelial cells by activating microglia and/or macrophages. Previous studies suggested that the reactive astrocytes are associated with the increase of Aβ plaque deposits. However, the Aβ plaque number has no significant difference in the cortex between *App*Tg and *App*Tg/*Cebpd*$^{-/-}$ mice (data not shown). It suggested that CEBPD may not involve in Aβ plaque deposition, but this speculation needs to be further investigated and verified. Our recent evidence suggested that the activation of astrocytic CEBPD plays a crucial role in AD pathogenesis as its activation is associated with the attenuation of phagocytosis (Ko et al., 2012), the promotion of microglia and macrophage migration (Ko et al., 2014), and angiogenesis (in the present study). These findings also imply that CEBPD could be a biomarker or therapeutic target for AD.

Disclosure statement

None of the authors has a conflict of interest to declare in relation to the present research.

Acknowledgements

This work was supported and fund for Open Access publication by grant MOST103-2321-B-006-031 and MOST103-2320-B-006-034-MY3 and also supported by a "New Partnership Program for the Connection to the Top Labs in the World" with Kyoto University (NSC101-2911-I-038–501) from the Ministry of Science and Technology, Taiwan.

Appendix A. Supplementary data

Supplementary data associated with this article can be found, in the online version, at http://dx.doi.org/10.1016/j.neurobiolaging.2014.11.020.

References

Adams, J.C., Lawler, J., 2004. The thrombospondins. Int. J. Biochem. Cell Biol. 36, 961–968.

Akiyama, H., Barger, S., Barnum, S., Bradt, B., Bauer, J., Cole, G.M., Cooper, N.R., Eikelenboom, P., Emmerling, M., Fiebich, B.L., Finch, C.E., Frautschy, S., Griffin, W.S., Hampel, H., Hull, M., Landreth, G., Lue, L., Mrak, R., Mackenzie, I.R., Mcgeer, P.L., O'banion, M.K., Pachter, J., Pasinetti, G., Plata-Salaman, C., Rogers, J., Rydel, R., Shen, Y., Streit, W., Strohmeyer, R., Tooyoma, I., Van Muiswinkel, F.L., Veerhuis, R., Walker, D., Webster, S., Wegrzyniak, B., Wenk, G., Wyss-Coray, T., 2000. Inflammation and Alzheimer's disease. Neurobiol. Aging 21, 383–421.

Asch, A.S., Leung, L.L., Shapiro, J., Nachman, R.L., 1986. Human brain glial cells synthesize thrombospondin. Proc. Natl. Acad. Sci. U. S. A. 83, 2904–2908.

Bennett, C.E., Nsengimana, J., Bostock, J.A., Cymbalista, C., Futers, T.S., Knight, B.L., Mccormack, L.J., Prasad, U.K., Riches, K., Rolton, D., Scarrott, T., Barrett, J.H., Carter, A.M., 2010. CCAAT/enhancer binding protein alpha, beta and delta gene variants: associations with obesity related phenotypes in the Leeds Family Study. Diab. Vasc. Dis. Res. 7, 195–203.

Berezikov, E., Thuemmler, F., Van Laake, L.W., Kondova, I., Bontrop, R., Cuppen, E., Plasterk, R.H., 2006. Diversity of microRNAs in human and chimpanzee brain. Nat. Genet. 38, 1375–1377.

Bergamaschini, L., Rossi, E., Storini, C., Pizzimenti, S., Distaso, M., Perego, C., De Luigi, A., Vergani, C., De Simoni, M.G., 2004. Peripheral treatment with enoxaparin, a low molecular weight heparin, reduces plaques and beta-amyloid accumulation in a mouse model of Alzheimer's disease. J. Neurosci. 24, 4181–4186.

Bezzi, P., Carmignoto, G., Pasti, L., Vesce, S., Rossi, D., Rizzini, B.L., Pozzan, T., Volterra, A., 1998. Prostaglandins stimulate calcium-dependent glutamate release in astrocytes. Nature 391, 281–285.

Biron, K.E., Dickstein, D.L., Gopaul, R., Jefferies, W.A., 2011. Amyloid triggers extensive cerebral angiogenesis causing blood brain barrier permeability and hypervascularity in Alzheimer's disease. PLoS One 6, e23789.

Blake, S.M., Strasser, V., Andrade, N., Duit, S., Hofbauer, R., Schneider, W.J., Nimpf, J., 2008. Thrombospondin-1 binds to ApoER2 and VLDL receptor and functions in postnatal neuronal migration. EMBO J. 27, 3069–3080.

Bornstein, P., 2001. Thrombospondins as matricellular modulators of cell function. J. Clin. Invest. 107, 929–934.

Buee, L., Hof, P.R., Roberts, D.D., Delacourte, A., Morrison, J.H., Fillit, H.M., 1992. Immunohistochemical identification of thrombospondin in normal human brain and in Alzheimer's disease. Am. J. Pathol. 141, 783–788.

Bueno, M.J., Perez De Castro, I., Malumbres, M., 2008. Control of cell proliferation pathways by microRNAs. Cell Cycle 7, 3143–3148.

Cardinaux, J.R., Allaman, I., Magistretti, P.J., 2000. Pro-inflammatory cytokines induce the transcription factors C/EBPbeta and C/EBPdelta in astrocytes. Glia 29, 91–97.

Chang, L.H., Huang, H.S., Wu, P.T., Jou, I.M., Pan, M.H., Chang, W.C., Wang, D.D., Wang, J.M., 2012. Role of macrophage CCAAT/enhancer binding protein delta in the pathogenesis of rheumatoid arthritis in collagen-induced arthritic mice. PLoS One 7, e45378.

Christopherson, K.S., Ullian, E.M., Stokes, C.C., Mullowney, C.E., Hell, J.W., Agah, A., Lawler, J., Mosher, D.F., Bornstein, P., Barres, B.A., 2005. Thrombospondins are astrocyte-secreted proteins that promote CNS synaptogenesis. Cell 120, 421–433.

Czirr, E., Wyss-Coray, T., 2012. The immunology of neurodegeneration. J. Clin. Invest. 122, 1156–1163.

De Jesus Perez, V.A., Alastalo, T.P., Wu, J.C., Axelrod, J.D., Cooke, J.P., Amieva, M., Rabinovitch, M., 2009. Bone morphogenetic protein 2 induces pulmonary angiogenesis via Wnt-beta-catenin and Wnt-RhoA-Rac1 pathways. J. Cell Biol. 184, 83–99.

Delghandi, M.P., Johannessen, M., Moens, U., 2005. The cAMP signalling pathway activates CREB through PKA, p38 and MSK1 in NIH 3T3 cells. Cell. Signal 17, 1343–1351.

Desai, B.S., Schneider, J.A., Li, J.L., Carvey, P.M., Hendey, B., 2009. Evidence of angiogenic vessels in Alzheimer's disease. J. Neural Transm. 116, 587–597.

Dews, M., Homayouni, A., Yu, D., Murphy, D., Sevignani, C., Wentzel, E., Furth, E.E., Lee, W.M., Enders, G.H., Mendell, J.T., Thomas-Tikhonenko, A., 2006. Augmentation of tumor angiogenesis by a Myc-activated microRNA cluster. Nat. Genet. 38, 1060–1065.

Fiala, M., Cribbs, D.H., Rosenthal, M., Bernard, G., 2007. Phagocytosis of amyloid-beta and inflammation: two faces of innate immunity in Alzheimer's disease. J. Alzheimers Dis. 11, 457–463.

Fiala, M., Lin, J., Ringman, J., Kermani-Arab, V., Tsao, G., Patel, A., Lossinsky, A.S., Graves, M.C., Gustavson, A., Sayre, J., Sofroni, E., Suarez, T., Chiappelli, F., Bernard, G., 2005. Ineffective phagocytosis of amyloid-beta by macrophages of Alzheimer's disease patients. J. Alzheimers Dis. 7, 221–232 discussion 255–262.

Fiebich, B.L., Schleicher, S., Spleiss, O., Czygan, M., Hull, M., 2001. Mechanisms of prostaglandin E2-induced interleukin-6 release in astrocytes: possible involvement of EP4-like receptors, p38 mitogen-activated protein kinase and protein kinase C. J. Neurochem. 79, 950–958.

Font-Nieves, M., Sans-Fons, M.G., Gorina, R., Bonfill-Teixidor, E., Salas-Perdomo, A., Marquez-Kisinousky, L., Santalucia, T., Planas, A.M., 2012. Induction of COX-2 enzyme and down-regulation of COX-1 expression by lipopolysaccharide (LPS) control prostaglandin E2 production in astrocytes. J. Biol. Chem. 287, 6454–6468.

Forette, F., Seux, M.L., Staessen, J.A., Thijs, L., Birkenhager, W.H., Babarskiene, M.R., Babeanu, S., Bossini, A., Gil-Extremera, B., Girerd, X., Laks, T., Lilov, E., Moisseyev, V., Tuomilehto, J., Vanhanen, H., Webster, J., Yodfat, Y., Fagard, R., 1998. Prevention of dementia in randomised double-blind placebo-controlled systolic hypertension in Europe (Syst-Eur) trial. Lancet 352, 1347–1351.

Garcia, K.O., Ornellas, F.L., Martin, P.K., Patti, C.L., Mello, L.E., Frussa-Filho, R., Han, S.W., Longo, B.M., 2014. Therapeutic effects of the transplantation of VEGF overexpressing bone marrow mesenchymal stem cells in the hippocampus of murine model of Alzheimer's disease. Front. Aging Neurosci. 6, 30.

Glass, C.K., Saijo, K., Winner, B., Marchetto, M.C., Gage, F.H., 2010. Mechanisms underlying inflammation in neurodegeneration. Cell 140, 918–934.

He, L., Hannon, G.J., 2004. MicroRNAs: small RNAs with a big role in gene regulation. Nat. Rev. Genet. 5, 522–531.

Hirata, T., Narumiya, S., 2011. Prostanoid receptors. Chem. Rev. 111, 6209–6230.

Ho, L., Purohit, D., Haroutunian, V., Luterman, J.D., Willis, F., Naslund, J., Buxbaum, J.D., Mohs, R.C., Aisen, P.S., Pasinetti, G.M., 2001. Neuronal cyclooxygenase 2 expression in the hippocampal formation as a function of the clinical progression of Alzheimer disease. Arch. Neurol. 58, 487–492.

Hoozemans, J.J., O'banion, M.K., 2005. The role of COX-1 and COX-2 in Alzheimer's disease pathology and the therapeutic potentials of non-steroidal anti-inflammatory drugs. Curr. Drug Targets CNS Neurol. Disord. 4, 307–315.

Hoshino, T., Namba, T., Takehara, M., Murao, N., Matsushima, T., Sugimoto, Y., Narumiya, S., Suzuki, T., Mizushima, T., 2012. Improvement of cognitive function in Alzheimer's disease model mice by genetic and pharmacological inhibition of the EP(4) receptor. J. Neurochem. 120, 795–805.

Hsiao, Y.W., Li, C.F., Chi, J.Y., Tseng, J.T., Chang, Y., Hsu, L.J., Lee, C.H., Chang, T.H., Wang, S.M., Wang, D.D., Cheng, H.C., Wang, J.M., 2013. CCAAT/enhancer binding protein delta in macrophages contributes to immunosuppression and inhibits phagocytosis in nasopharyngeal carcinoma. Sci. Signal 6, ra59.

Hsiao, H.Y., Mak, O.T., Yang, C.S., Liu, Y.P., Fang, K.M., Tzeng, S.F., 2007. TNF-alpha/IFN-gamma-induced iNOS expression increased by prostaglandin E2 in rat primary astrocytes via EP2-evoked cAMP/PKA and intracellular calcium signaling. Glia 55, 214–223.

Ikonomovic, M.D., Uryu, K., Abrahamson, E.E., Ciallella, J.R., Trojanowski, J.Q., Lee, V.M., Clark, R.S., Marion, D.W., Wisniewski, S.R., Dekosky, S.T., 2004. Alzheimer's pathology in human temporal cortex surgically excised after severe brain injury. Exp. Neurol. 190, 192–203.

Imbimbo, B.P., Solfrizzi, V., Panza, F., 2010. Are NSAIDs useful to treat Alzheimer's disease or mild cognitive impairment? Front. Aging Neurosci. 2, 19–32.

in 't Veld, B.A., Ruitenberg, A., Hofman, A., Launer, L.J., Van Duijn, C.M., Stijnen, T., Breteler, M.M., Stricker, B.H., 2001. Nonsteroidal antiinflammatory drugs and the risk of Alzheimer's disease. N. Engl. J. Med. 345, 1515–1521.

Jander, S., Schroeter, M., D'urso, D., Gillen, C., Witte, O.W., Stoll, G., 1998. Focal ischaemia of the rat brain elicits an unusual inflammatory response: early appearance of CD8+ macrophages/microglia. Eur. J. Neurosci. 10, 680–688.

Jantaratnotai, N., Schwab, C., Ryu, J.K., Mcgeer, P.L., Mclarnon, J.G., 2010. Converging perturbed microvasculature and microglial clusters characterize Alzheimer disease brain. Curr. Alzheimer Res. 7, 625–636.

Jesmin, S., Sakuma, I., Hattori, Y., Fujii, S., Kitabatake, A., 2002. Long-acting calcium channel blocker benidipine suppresses expression of angiogenic growth factors and prevents cardiac remodelling in a type II diabetic rat model. Diabetologia 45, 402–415.

Jick, H., Zornberg, G.L., Jick, S.S., Seshadri, S., Drachman, D.A., 2000. Statins and the risk of dementia. Lancet 356, 1627–1631.

Jones, M.K., Wang, H., Peskar, B.M., Levin, E., Itani, R.M., Sarfeh, I.J., Tarnawski, A.S., 1999. Inhibition of angiogenesis by nonsteroidal anti-inflammatory drugs: insight into mechanisms and implications for cancer growth and ulcer healing. Nat. Med. 5, 1418–1423.

Kabashima, K., Saji, T., Murata, T., Nagamachi, M., Matsuoka, T., Segi, E., Tsuboi, K., Sugimoto, Y., Kobayashi, T., Miyachi, Y., Ichikawa, A., Narumiya, S., 2002. The prostaglandin receptor EP4 suppresses colitis, mucosal damage and CD4 cell activation in the gut. J. Clin. Invest. 109, 883–893.

Kanwar, J.R., Mahidhara, G., Kanwar, R.K., 2010. MicroRNA in human cancer and chronic inflammatory diseases. Front. Biosci. (Schol Ed) 2, 1113–1126.

Kitamura, Y., Shimohama, S., Koike, H., Kakimura, Ji, Matsuoka, Y., Nomura, Y., Gebicke-Haerter, P.J., Taniguchi, T., 1999. Increased expression of cyclooxygenases and peroxisome proliferator-activated receptor-gamma in Alzheimer's disease brains. Biochem. Biophys. Res. Commun. 254, 582–586.

Ko, C.Y., Chang, L.H., Lee, Y.C., Sterneck, E., Cheng, C.P., Chen, S.H., Huang, A.M., Tseng, J.T., Wang, J.M., 2012. CCAAT/enhancer binding protein delta (CEBPD) elevating PTX3 expression inhibits macrophage-mediated phagocytosis of dying neuron cells. Neurobiol. Aging 33, 422 e11–25.

Ko, C.Y., Wang, W.L., Wang, S.M., Chu, Y.Y., Chang, W.C., Wang, J.M., 2014. Glycogen synthase kinase-3beta-mediated CCAAT/enhancer-binding protein delta phosphorylation in astrocytes promot es migration and activation of microglia/macrophages. Neurobiol. Aging 35, 24–34.

Landgraf, P., Rusu, M., Sheridan, R., Sewer, A., Iovino, N., Aravin, A., Pfeffer, S., Rice, A., Kamphorst, A.O., Landthaler, M., Lin, C., Socci, N.D., Hermida, L., Fulci, V., Chiaretti, S., Foa, R., Schliwka, J., Fuchs, U., Novosel, A., Muller, R.U., Schermer, B., Bissels, U., Inman, J., Phan, Q., Chien, M., Weir, D.B., Choksi, R., De Vita, G., Frezzetti, D., Trompeter, H.I., Hornung, V., Teng, G., Hartmann, G., Palkovits, M., Di Lauro, R., Wernet, P., Macino, G., Rogler, C.E., Nagle, J.W., Ju, J., Papavasiliou, F.N., Benzing, T., Lichter, P., Tam, W., Brownstein, M.J., Bosio, A., Borkhardt, A., Russo, J.J., Sander, C., Zavolan, M., Tuschl, T., 2007. A mammalian microRNA expression atlas based on small RNA library sequencing. Cell 129, 1401–1414.

Lau, P., De Strooper, B., 2010. Dysregulated microRNAs in neurodegenerative disorders. Semin. Cell Dev. Biol. 21, 768–773.

Leahy, K.M., Koki, A.T., Masferrer, J.L., 2000. Role of cyclooxygenases in angiogenesis. Curr. Med. Chem. 7, 1163–1170.

Lee, S.T., Chu, K., Jung, K.H., Kim, J.H., Huh, J.Y., Yoon, H., Park, D.K., Lim, J.Y., Kim, J.M., Jeon, D., Ryu, H., Lee, S.K., Kim, M., Roh, J.K., 2012. miR-206 regulates brain-derived neurotrophic factor in Alzheimer disease model. Ann. Neurol. 72, 269–277.

Lee, C.Y., Landreth, G.E., 2010. The role of microglia in amyloid clearance from the AD brain. J. Neural Transm. 117, 949–960.

Li, R., Strohmeyer, R., Liang, Z., Lue, L.F., Rogers, J., 2004. CCAAT/enhancer binding protein delta (C/EBPdelta) expression and elevation in Alzheimer's disease. Neurobiol. Aging 25, 991–999.

Manoonkitiwongsa, P.S., Jackson-Friedman, C., Mcmillan, P.J., Schultz, R.L., Lyden, P.D., 2001. Angiogenesis after stroke is correlated with increased numbers of macrophages: the clean-up hypothesis. J. Cereb. Blood Flow Metab. 21, 1223–1231.

Mcgeer, P.L., Mcgeer, E., Rogers, J., Sibley, J., 1990. Anti-inflammatory drugs and Alzheimer disease. Lancet 335, 1037.

Milner, R., Campbell, I.L., 2002. Cytokines regulate microglial adhesion to laminin and astrocyte extracellular matrix via protein kinase C-dependent activation of the alpha6beta1 integrin. J. Neurosci. 22, 1562–1572.

Montine, T.J., Sidell, K.R., Crews, B.C., Markesbery, W.R., Marnett, L.J., Roberts 2nd, L.J., Morrow, J.D., 1999. Elevated CSF prostaglandin E2 levels in patients with probable AD. Neurology 53, 1495–1498.

Narumiya, S., Fitzgerald, G.A., 2001. Genetic and pharmacological analysis of prostanoid receptor function. J. Clin. Invest. 108, 25–30.

Neugebauer, K.M., Emmett, C.J., Venstrom, K.A., Reichardt, L.F., 1991. Vitronectin and thrombospondin promote retinal neurite outgrowth: developmental regulation and role of integrins. Neuron 6, 345–358.

Nishimura, Y., Nitto, T., Inoue, T., Node, K., 2008. IL-13 attenuates vascular tube formation via JAK2-STAT6 pathway. Circ. J. 72, 469–475.

O'shea, K.S., Liu, L.H., Dixit, V.M., 1991. Thrombospondin and a 140 kd fragment promote adhesion and neurite outgrowth from embryonic central and peripheral neurons and from PC12 cells. Neuron 7, 231–237.

Osterhout, D.J., Frazier, W.A., Higgins, D., 1992. Thrombospondin promotes process outgrowth in neurons from the peripheral and central nervous systems. Dev. Biol. 150, 256–265.

Perlmutter, L.S., Chui, H.C., Saperia, D., Athanikar, J., 1990. Microangiopathy and the colocalization of heparan sulfate proteoglycan with amyloid in senile plaques of Alzheimer's disease. Brain Res. 508, 13–19.

Polverini, P.J., Cotran, P.S., Gimbrone Jr., M.A., Unanue, E.R., 1977. Activated macrophages induce vascular proliferation. Nature 269, 804–806.

Rama Rao, K.V., Curtis, K.M., Johnstone, J.T., Norenberg, M.D., 2013. Amyloid-beta inhibits thrombospondin 1 release from cultured astrocytes: effects on synaptic protein expression. J. Neuropathol. Exp. Neurol. 72, 735–744.
Ramji, D.P., Foka, P., 2002. CCAAT/enhancer-binding proteins: structure, function and regulation. Biochem. J. 365, 561–575.
Ramji, D.P., Vitelli, A., Tronche, F., Cortese, R., Ciliberto, G., 1993. The two C/EBP isoforms, IL-6DBP/NF-IL6 and C/EBP delta/NF-IL6 beta, are induced by IL-6 to promote acute phase gene transcription via different mechanisms. Nucleic Acids Res. 21, 289–294.
Salcedo, R., Zhang, X., Young, H.A., Michael, N., Wasserman, K., Ma, W.H., Martins-Green, M., Murphy, W.J., Oppenheim, J.J., 2003. Angiogenic effects of prostaglandin E2 are mediated by up-regulation of CXCR4 on human microvascular endothelial cells. Blood 102, 1966–1977.
Samols, M.A., Skalsky, R.L., Maldonado, A.M., Riva, A., Lopez, M.C., Baker, H.V., Renne, R., 2007. Identification of cellular genes targeted by KSHV-encoded microRNAs. PLoS Pathog. 3, e65.
Scott-Drew, S., Ffrench-Constant, C., 1997. Expression and function of thrombospondin-1 in myelinating glial cells of the central nervous system. J. Neurosci. Res. 50, 202–214.
Simard, A.R., Soulet, D., Gowing, G., Julien, J.P., Rivest, S., 2006. Bone marrow-derived microglia play a critical role in restricting senile plaque formation in Alzheimer's disease. Neuron 49, 489–502.
Song, H.S., Son, M.J., Lee, Y.M., Kim, W.J., Lee, S.W., Kim, C.W., Kim, K.W., 2002. Oxygen tension regulates the maturation of the blood-brain barrier. Biochem. Biophys. Res. Commun. 290, 325–331.
Sonntag, K.C., 2010. MicroRNAs and deregulated gene expression networks in neurodegeneration. Brain Res. 1338, 48–57.
Sterneck, E., Paylor, R., Jackson-Lewis, V., Libbey, M., Przedborski, S., Tessarollo, L., Crawley, J.N., Johnson, P.F., 1998. Selectively enhanced contextual fear conditioning in mice lacking the transcriptional regulator CCAAT/enhancer binding protein delta. Proc. Natl. Acad. Sci. U. S. A. 95, 10908–10913.
Suzawa, T., Miyaura, C., Inada, M., Maruyama, T., Sugimoto, Y., Ushikubi, F., Ichikawa, A., Narumiya, S., Suda, T., 2000. The role of prostaglandin E receptor subtypes (EP1, EP2, EP3, and EP4) in bone resorption: an analysis using specific agonists for the respective EPs. Endocrinology 141, 1554–1559.
Thounaojam, M.C., Kaushik, D.K., Basu, A., 2013. MicroRNAs in the brain: it's regulatory role in neuroinflammation. Mol. Neurobiol. 47, 1034–1044.
Tran, M.D., Neary, J.T., 2006. Purinergic signaling induces thrombospondin-1 expression in astrocytes. Proc. Natl. Acad. Sci. U. S. A. 103, 9321–9326.
Vagnucci Jr., A.H., Li, W.W., 2003. Alzheimer's disease and angiogenesis. Lancet 361, 605–608.
Wang, J.M., Ko, C.Y., Chen, L.C., Wang, W.L., Chang, W.C., 2006. Functional role of NF-IL6beta and its sumoylation and acetylation modifications in promoter activation of cyclooxygenase 2 gene. Nucleic Acids Res. 34, 217–231.
Wang, J.M., Tseng, J.T., Chang, W.C., 2005. Induction of human NF-IL6beta by epidermal growth factor is mediated through the p38 signaling pathway and cAMP response element-binding protein activation in A431 cells. Mol. Biol. Cell 16, 3365–3376.
Waschbisch, A., Fiebich, B.L., Akundi, R.S., Schmitz, M.L., Hoozemans, J.J., Candelario-Jalil, E., Virtainen, N., Veerhuis, R., Slawik, H., Yrjanheikki, J., Hull, M., 2006. Interleukin-1 beta-induced expression of the prostaglandin E-receptor subtype EP3 in U373 astrocytoma cells depends on protein kinase C and nuclear factor-kappaB. J. Neurochem. 96, 680–693.
Welser, J.V., Li, L., Milner, R., 2010. Microglial activation state exerts a biphasic influence on brain endothelial cell proliferation by regulating the balance of TNF and TGF-beta1. J. Neuroinflammation 7, 89.
Wu, S., Lin, Y., Xu, D., Chen, J., Shu, M., Zhou, Y., Zhu, W., Su, X., Zhou, Y., Qiu, P., Yan, G., 2012. MiR-135a functions as a selective killer of malignant glioma. Oncogene 31, 3866–3874.
Wyss-Coray, T., 2006. Inflammation in Alzheimer disease: driving force, bystander or beneficial response? Nat. Med. 12, 1005–1015.
Xu, J., Chalimoniuk, M., Shu, Y., Simonyi, A., Sun, A.Y., Gonzalez, F.A., Weisman, G.A., Wood, W.G., Sun, G.Y., 2003. Prostaglandin E2 production in astrocytes: regulation by cytokines, extracellular ATP, and oxidative agents. Prostaglandins Leukot. Essent. Fatty Acids 69, 437–448.
Yamaji-Kegan, K., Su, Q., Angelini, D.J., Johns, R.A., 2009. IL-4 is proangiogenic in the lung under hypoxic conditions. J. Immunol. 182, 5469–5476.
Yang, X., Castilla, L.H., Xu, X., Li, C., Gotay, J., Weinstein, M., Liu, P.P., Deng, C.X., 1999. Angiogenesis defects and mesenchymal apoptosis in mice lacking SMAD5. Development 126, 1571–1580.
Yang, Z.H., Kitami, Y., Takata, Y., Okura, T., Hiwada, K., 2001. Targeted overexpression of CCAAT/enhancer-binding protein-delta evokes enhanced gene transcription of platelet-derived growth factor alpha-receptor in vascular smooth muscle cells. Circ. Res. 89, 503–508.
Yu, H., Kumar, P.P., 2003. Post-transcriptional gene silencing in plants by RNA. Plant Cell Rep. 22, 167–174.
Zekry, D., Duyckaerts, C., Moulias, R., Belmin, J., Geoffre, C., Herrmann, F., Hauw, J.J., 2002. Degenerative and vascular lesions of the brain have synergistic effects in dementia of the elderly. Acta Neuropathol. 103, 481–487.
Zhang, Y., Daaka, Y., 2011. PGE2 promotes angiogenesis through EP4 and PKA Cgamma pathway. Blood 118, 5355–5364.